A possible influence of extracellular polysaccharides on the analysis of intracellular metabolites from Trichoderma harzianum grown under carbon-limited conditions

Gelain, Lucas; Geraldo da Cruz Pradella, José; Carvalho da Costa, Aline; van der Wielen, Luuk; van Gulik, Walter M.

DOI
10.1016/j.funbio.2020.12.002

Publication date
2021

Document Version
Final published version

Published in
Fungal Biology

Citation (APA)
Gelain, L., Geraldo da Cruz Pradella, J., Carvalho da Costa, A., van der Wielen, L., & van Gulik, W. M. (2021). A possible influence of extracellular polysaccharides on the analysis of intracellular metabolites from Trichoderma harzianum grown under carbon-limited conditions. *Fungal Biology*, *125*(5), 368-377. https://doi.org/10.1016/j.funbio.2020.12.002

Fungal Biology 125 (2021) 368–377

Contents lists available at ScienceDirect

Fungal Biology

journal homepage: www.elsevier.com/locate/funbio

A possible influence of extracellular polysaccharides on the analysis of intracellular metabolites from *Trichoderma harzianum* grown under carbon-limited conditions

Lucas Gelain [a, b, *], José Geraldo da Cruz Pradella [d], Aline Carvalho da Costa [b], Luuk van der Wielen [a, c], Walter M. van Gulik [a]

[a] Delft University of Technology, Department of Biotechnology, Van der Maasweg 9, 2629HZ, Delft, the Netherlands
[b] University of Campinas, School of Chemical Engineering, Av. Albert Einstein, 500, Campinas, Brazil
[c] University of Limerick, Bernal Institute, V94 T9PX, Limerick, Ireland
[d] Federal University of São Paulo, Institute of Science and Technology, Av. Cesare Mansueto Giulio Lattes, 1201, S. J. Campos, Brazil

ARTICLE INFO

Article history:
Received 26 April 2020
Received in revised form
30 October 2020
Accepted 8 December 2020
Available online 11 December 2020

Corresponding editor: Prof. G.M. Gadd

Keywords:
Continuous culture
Carbon limitation
Metabolites
Fragments from extracellular polysaccharides

ABSTRACT

Intracellular metabolites were evaluated during the continuous growth of *Trichoderma harzianum* P49P11 under carbon-limited conditions. Four different conditions in duplicate were investigated (10 and 20 g/L of glucose, 5.26/5.26 g/L of fructose/glucose and 10 g/L of sucrose in the feed). Differences in the values of some specific concentrations of intracellular metabolites were observed at steady-state for the duplicates. The presence of extracellular polysaccharide was confirmed in the supernatant of all conditions based on FT-IR and proton NMR. Fragments of polysaccharides from the cell wall could be released due to the shear stress and since the cells can consume them under carbon-limited conditions, this could create an unpredictable carbon flow rate into the cells. According to the values of the metabolite concentrations, it was considered that the consumption of those fragments was interfering with the analysis.

1. Introduction

The quantitative analysis of metabolites is a prerequisite for metabolic engineering (Buchholz et al., 2001), which can be applied to create an optimal strain to produce desired products. *T. harzianum* P49P11 has been applied to produce enzymes that can convert lignocellulosic polymers into their monomers (Delabona et al., 2013; Gelain et al., 2015) and to date, no analysis of intracellular metabolites has been described in the literature for this wild strain. Thus, studies to evaluate the quantitative analysis of metabolites employing *T. harzianum* P49P11 is the first step for the development of an optimal strain through metabolic engineering.

The analysis of the intracellular metabolites of a microorganism involves the following steps: the cell growth under specific conditions; sampling and quenching of the cells; extraction and analysis of the metabolites (Pinu et al., 2017). Quenching methods are used to stop the cell metabolism, which is required to evaluate the metabolic behaviour of the cells under a specific condition. According to Pinu et al. (2017), the majority of the quenching methods were developed for bacteria and/or yeast, and a few quenching methods have been reported for filamentous fungi. Jonge et al. (2012) evaluated and optimized a sampling procedure for quantitative metabolomics based on cold aqueous methanol quenching using *Penicillium chrysogenum* DS17690, glucose as the limiting substrate and the dilution rate of 0.05 h^{-1}. They optimized the method to reduce leakage and found that metabolite leakage was minimal for a methanol content of the quenching solution of 40% (v/v) at −25 °C. Lameiras et al. (2015) described a quenching method for quantitative metabolomics aiming to avoid metabolite leakage during sample processing employing *Aspergillus niger* NW185 on glucose-limited conditions with dilution rates of 0.043 and 0.089 h^{-1}. They found that the leakage was absent at −20 °C for 40% (v/v) methanol solution. The method described in Lameiras

* Corresponding author. Delft University of Technology, Department of Biotechnology, Van der Maasweg 9, 2629HZ, Delft, the Netherlands.
E-mail addresses: lgelain@ucs.br, lucas26gelain@hotmail.com (L. Gelain).

https://doi.org/10.1016/j.funbio.2020.12.002

Table 1
Intracellular metabolites of glycolysis and extracellular glucose (m, μmol/g), experimental errors (e, %) and the difference in the specific concentration of the metabolite regarding the average of the group (D_m, %), metabolites with significantly different levels for the duplicates are indicated in blue (Tukey test with 95% confidence interval).

Conditions	Extracellular glucose			Glucose			Glucose-6-phosphate		
	m	e	D_m	m	e	D_m	m	e	D_m
G101	1.220	±19.3	9.6	2.029	±21.4	12.8	1.737	±15.3	1.4
G102	2.392	±17.4	29.2	5.018	±19.9	41.9	1.737	±12.9	1.4
G201	1.742	±15.7	7.7	1.184	±31.7	28.3	1.393	±1.7	8.8
G202	0.683	±3.8	27.4	2.689	±54.5	0.8	1.895	±5.4	6.0
FG1	0.790	±31.8	26	1.655	±22.9	31.2	1.100	±5.1	20.2
FG2	0.583	±41.3	32.3	9.460	±64.3	57.5	1.820	±10.9	0.7
S1	1.469	±7.0	5.4	4.030	±28.3	4.2	1.753	±0.3	2.6
S2	3.746	±21.5	63.7	2.456	±5.9	22.1	2.716	±8.1	23.5

Conditions	Fructose-6-phosphate			Fructose-1,6-bisphosphate			Glyceraldehyde-3-phosphate		
	m	e	D_m	m	e	D_m	m	e	D_m
G101	0.323	±15.5	2.4	0.351	±7.7	0.9	0.017	±19.9	4.5
G102	0.388	±12.9	7.1	0.407	±26.2	6.9	0.024	±19.8	14.7
G201	0.279	±7.0	8.9	0.403	±1.9	6.3	0.024	±8.5	15.1
G202	0.368	±2.0	4.2	0.269	±16.4	12.4	0.009	±4.3	25.3
FG1	0.265	±2.8	19.2	0.338	±6.4	14.5	0.017	±4.0	7.8
FG2	0.511	±11.6	9.5	0.343	±3.3	14.0	0.014	±7.5	15.2
S1	0.310	±16.0	13.9	0.416	±17.0	6.3	0.016	±35.5	9.4
S2	0.633	±6.6	23.6	0.807	±4.1	34.8	0.033	±18.4	32.4

Conditions	Dihydroxyacetone phosphate			3-Phosphoglycerate			2-Phosphoglycerate		
	m	e	D_m	m	e	D_m	m	e	D_m
G101	0.123	±5.9	6.3	0.449	±18.1	5.1	0.041	±18.8	7.2
G102	0.184	±16.0	15.1	0.442	±3.7	5.8	0.044	±4.5	4.9
G201	0.139	±10.4	0.8	0.476	±4.2	2.3	0.050	±8.3	1.9
G202	0.119	±1.5	8.0	0.632	±17.9	13.2	0.058	±17.5	10.1
FG1	0.132	±4.0	12.1	0.487	±6.5	12.5	0.044	±8.5	15.0
FG2	0.160	±1.1	4.0	0.477	±8.2	13.2	0.050	±7.1	9.8
S1	0.121	±6.9	15.2	0.938	±31.1	22.3	0.086	±32.6	18.3
S2	0.283	±12.2	31.3	0.692	±7.9	3.4	0.071	±9.1	6.6

Conditions	Phosphoenolpyruvate		
	m	e	D_m
G101	0.030	±20.1	10.5
G102	0.011	±6.2	27.9
G201	0.017	±0.8	16.2
G202	0.042	±68.9	33.6
FG1	0.043	±25.0	11.3
FG2	0.030	±30.6	23.3
S1	0.078	±41.2	19.8
S2	0.073	±6.9	14.8

et al. (2015) was used in this work for the first evaluation of intracellular metabolites from *T. harzianum* P49P11.

Extracellular polysaccharides have several applications in industries, in different product areas such as pharmaceuticals, medicine and foods. Despite their importance, information about fungal polysaccharide synthesis is scarce and an extensive search for new fungal species that can produce novel extracellular polysaccharides is still needed (Mahapatra and Banerjee, 2013). According to Gientka et al. (2015), some extracellular polysaccharides of yeasts show antitumor, immunostimulatory and antioxidant activity.

Trichoderma species are recognized for their high extracellular enzyme production but there are limited reports on the production of polysaccharides (Li et al., 2017). Li et al. (2017) evaluated *in vitro* the antitumor properties of an extracellular polysaccharide from *Trichoderma* sp. KK19L1 on human cervical carcinoma cells and human breast carcinoma cells. They have shown the potential of extracellular polysaccharides from *Trichoderma* sp to inhibit cancer cells.

The work aims to evaluate the specific concentrations of intracellular metabolites under carbon-limited conditions. The production of extracellular polysaccharides by *T. harzianum* P49P11 was discovered in this work and their presence in the growth medium could be interfering with the analysis. A method to evaluate the metabolic profiles optimized for a different microorganism (*Aspergillus niger* NW185, Lameiras et al., 2015) was used as the first step for the optimization of the analysis employing *T. harzianum*.

Table 2
Nucleotides (m, μmol/g), experimental errors (e, %) and the difference in the specific concentration of the nucleotide regarding the average of the group (D_m, %), nucleotides with significantly different levels for the duplicates are indicated in blue (Tukey test with 95% confidence interval).

Conditions	Adenosine monophosphate			Adenosine diphosphate			Adenosine triphosphate		
	m	e	D_m	m	e	D_m	m	e	D_m
G101	0.163	±10.1	25.7	0.980	±5.2	6.3	3.386	±5.6	9.8
G102	0.294	±24.4	6.1	0.879	±1.1	10.8	2.737	±5.9	1.7
G201	0.411	±20.2	11.4	0.879	±8.7	10.8	2.642	±14.0	3.4
G202	0.470	±11.9	20.3	1.745	±8.4	27.8	2.560	±15.6	4.8
FG1	0.160	±43.6	26.3	0.825	±7.8	12.8	2.573	±9.8	8.5
FG2	0.361	±9.6	3.5	1.345	±8.8	10.6	3.353	±0.1	8.4
S1	0.355	±3.9	2.6	1.225	±5.1	5.2	2.925	±4.0	1.5
S2	0.473	±6.2	20.1	1.044	±10.9	3.0	3.539	±0.9	11.4
Conditions	**Uridine monophosphate**			**Uridine diphosphate**			**Uridine triphosphate**		
	m	e	D_m	m	e	D_m	m	e	D_m
G101	0.058	±11.3	8.5	0.146	±4.3	10.8	0.658	±3.5	11.0
G102	0.065	±14.6	3.4	0.097	±6.2	9.6	0.440	±12.7	9.3
G201	0.069	±7.1	0.6	0.099	±6.0	9.0	0.464	±16.0	7.0
G202	0.087	±26.2	12.5	0.139	±16.0	7.7	0.596	±24.4	5.3
FG1	0.117	±65.4	19.7	0.126	±8.7	4.1	0.520	±5.0	11.8
FG2	0.105	±41.5	12.9	0.144	±45.7	2.5	0.965	±30.4	21.0
S1	0.083	±26.1	0.4	0.148	±12.8	4.0	0.601	±11.6	5.8
S2	0.030	±49.6	32.2	0.130	±7.6	2.4	0.632	±2.9	3.5
Conditions	**Guanosine monophosphate**			**Guanosine diphosphate**			**Guanosine triphosphate**		
	m	e	D_m	m	e	D_m	m	e	D_m
G101	0.152	±9.7	0.4	0.233	±7.3	7.2	0.872	±7.7	9.4
G102	0.094	±30.8	19.5	0.221	±5.2	4.2	0.679	±7.0	3.8
G201	0.111	±25.9	13.7	0.191	±10.6	3.1	0.607	±8.9	8.7
G202	0.257	±34.2	33.6	0.170	±19.9	8.2	0.780	±26.7	3.1
FG1	0.336	±74.1	22.7	0.207	±6.6	0.4	0.689	±1.9	11.6
FG2	0.140	±36.6	19.8	0.183	±40.5	6.1	1.248	±27.0	19.6
S1	0.314	±64.3	17.9	0.218	±13.7	2.1	0.800	±3.4	5.4
S2	0.135	±13.5	20.8	0.227	±4.1	4.3	0.847	±5.5	2.7

This method was used to verify the challenges imposed by the cell growth cultures using *T. harzianum* P49P11 on the analysis of intracellular metabolites under carbon-limited conditions.

2. Materials and methods

2.1. Culture conditions

Trichoderma harzianum P49P11 was isolated from the Amazon forest (Delabona et al., 2012). It was grown on potato dextrose agar at 29 °C and the spores were harvested after 5–7 days with sterilized water. The spore solutions were kept in stock at −80 °C. Culture conditions are also described in Gelain (2020). Spores from *T. harzianum* were used to inoculate 500 mL shake flasks containing 250 mL of the medium: 10 g/L of glucose (carbon source), 2 g/L of KH_2PO_4, 5 g/L of $(NH_4)_2SO_4$, 0.3 g/L of $MgSO_4.7H_2O$, 0.3 g/L of $CaCl_2.2H_2O$, 1 mL/L of trace elements solution, and 1 g/L of peptone. Trace elements solution: 15 g/L of $Na_2EDTA.2H_2O$, 4.5 g/L of $ZnSO_4.7H_2O$, 1 g/L of $MnCl_2.4H_2O$, 0.3 g/L of $CoCl_2.6H_2O$, 0.3 g/L of $CuSO_4.5H_2O$, 0.4 g/L of $Na_2MoO_4.2H_2O$, 4.5 g/L of $CaCl_2.2H_2O$, 3 g/L of $FeSO_4.7H_2O$, 1 g/L of H_3BO_3, 0.1 g/L of KI. The medium was sterilized at 121 °C for 20 min. The shake flasks were incubated in an orbital shaker for 24–48 h at 29 °C and 200 rpm before inoculating the bioreactor (10% v/v).

Different conditions were applied in carbon-limited chemostat cultures: 10 g/L of glucose (G101 and G102), 10 g/L of sucrose (S1 and S2), 5.26 and 5.26 g/L of fructose and glucose (FG1 and FG2). The medium composition was the same as described for shake flasks, only peptone was not added to the feed medium. Additionally, 20 g/L of glucose was also tested in the feed (G201 and G202) with the following modifications to the medium composition: 3 g/L of KH_2PO_4; and 6 g/L of $(NH_4)_2SO_4$. These alterations were made to maintain the same residual concentrations of these compounds in the effluent as for the condition using 10 g/L of glucose. The chemostat cultivations were performed in duplicate. The medium was sterilized by filtration using a filter 0.2 μm. The medium composition used for the batch stage was the same as used for the shake flask cultivation, except for the first batch experiment in which 20 g/L of sucrose was used as the carbon source. The medium for the batch stage was sterilized by filtration using a filter 0.2 μm.

A 7 L bioreactor (Applikon, Delft, the Netherlands) was used for the experiments with a constant broth mass of 4 kg. The temperature was controlled by a water bath at 29 °C, and pH 5 was controlled by the addition of 2 M KOH and 2 M H_2SO_4. Sterile air was supplied via a mass flow controller (Brooks 58505, calibration at 0 °C and 1 bar). The volume fraction of oxygen and carbon dioxide were measured by the NGA 2000 off-gas analyser.

Table 3
Intracellular metabolites of pentose phosphate pathway and citric acid cycle (m, μmol/g), experimental errors (e, %) and the difference in the specific concentration of the metabolite regarding the average of the group (D_m, %), metabolites with significantly different levels for the duplicates are indicated in blue (Tukey test with 95% confidence interval).

Conditions	6-Phosphogluconate			Ribulose-5-phosphate			Ribose-5-phosphate		
	m	e	D_m	m	e	D_m	m	e	D_m
G101	1.053	±29.9	19.8	0.080	±18.8	15.7	0.323	±8.3	1.2
G102	0.680	±11.3	4.9	0.164	±37.6	20.5	0.378	±21.6	10.0
G201	0.662	±6.6	6.1	0.183	±20.9	28.6	0.356	±8.4	6.5
G202	0.622	±18.4	8.8	0.038	±15.9	33.5	0.204	±1.3	17.7
FG1	1.075	±8.3	9.4	0.079	±21.3	19.6	0.246	±0.8	13.3
FG2	1.325	±3.4	0.1	0.123	±7.7	2.8	0.339	±4.7	0.6
S1	0.820	±14.8	19.0	0.096	±38.7	13.0	0.331	±31.7	0.6
S2	2.075	±2.4	28.4	0.222	±17.3	35.4	0.423	±12.7	13.2
Conditions	**Xylulose-5-phosphate**			**Sedoheptulose-7-phosphate**			**Erythrose-4-phosphate**		
	m	e	D_m	m	e	D_m	m	e	D_m
G101	0.154	±17.0	13.0	0.467	±20.6	1.1	0.0037	±9.2	1.9
G102	0.297	±47.0	21.3	0.536	±17.6	6.2	0.0045	±23.5	12.5
G201	0.300	±18.9	22.1	0.418	±6.0	6.2	0.0045	±8.8	12.8
G202	0.081	±0.5	30.5	0.488	±6.9	1.1	0.0016	±24.7	27.2
FG1	0.138	±16.6	19.5	0.358	±5.6	18.6	0.0028	±10.5	16.8
FG2	0.229	±9.8	0.7	0.580	±5.8	0.9	0.0036	±2.3	7.2
S1	0.172	±12.3	11.8	0.579	±6.3	0.8	0.0046	±34.7	4.5
S2	0.364	±12.3	30.6	0.763	±4.9	16.9	0.0059	±4.4	19.5
Conditions	**Citrate**			**Isocitrate**			**α-Ketoglutarate**		
	m	e	D_m	m	e	D_m	m	e	D_m
G101	12.49	±16.6	5.2	0.237	±34.0	2.1	0.424	±21.4	12.3
G102	14.41	±7.4	1.7	0.201	±8.2	5.7	0.514	±11.0	4.2
G201	12.08	±8.3	6.7	0.265	±5.1	8.3	0.606	±7.2	3.9
G202	16.79	±3.4	10.2	0.205	±21.6	4.8	0.703	±18.2	12.6
FG1	18.75	±3.0	17.5	0.355	±3.0	38.8	0.523	±1.6	11.0
FG2	10.31	±6.6	12.9	0.158	±6.7	10.3	0.920	±10.7	18.7
S1	15.24	±3.4	4.9	0.119	±35.7	20.3	0.443	±6.5	17.0
S2	11.26	±11.2	9.5	0.167	±2.8	8.2	0.793	±6.9	9.2
Conditions	**Succinate**			**Fumarate**			**Malate**		
	m	e	D_m	m	e	D_m	m	e	D_m
G101	1.804	±9.6	34.6	1.021	±9.4	4.0	1.810	±15.1	13.4
G102	0.845	±42.5	10.4	1.110	±12.3	8.7	2.339	±16.5	2.7
G201	0.901	±26.9	7.7	0.877	±10.6	3.6	2.811	±7.9	6.8
G202	0.714	±18.8	16.5	0.771	±7.6	9.2	2.937	±13.3	9.4
FG1	2.408	±9.0	26.1	0.950	±1.5	6.7	2.578	±4.6	8.1
FG2	0.586	±19.1	31.5	0.984	±5.2	5.2	3.014	±2.5	1.0
S1	2.647	±22.4	33.7	1.053	±8.0	2.0	2.938	±13.6	2.3
S2	0.687	±9.2	28.3	1.402	±16.5	13.9	3.782	±7.6	11.4

A dilution rate of 0.05 h^{-1} ±0.003 h^{-1} was used. For the batch stage, the stirring speed was kept between 200 and 400 rpm and for the continuous culture, it was changed to a constant stirring speed of 600 rpm. The airflow of 1 L/min was used, and only for the condition using 20 g/L of glucose, the airflow was 1.5 L/min. A constant antifoam addition (Basildon BC antifoam 86/013) of approximately 7 μL/min was used. The achievement of the steady-state was assumed when the CO_2 production and mycelium concentration were constant for at least 6 residence times.

2.2. Qualitative analysis of polysaccharides

Culture supernatant was obtained by filtration of the chemostat culture broth through 0.45 μm pore size filters (Millex-HV durapore PVDF membrane). Ethanol precipitation was performed by mixing 1 mL of the sample with 3 mL of pure ethanol. After centrifugation at 2000x g for 5 min, the precipitate was solubilized with 1 mL of water and precipitated again with 3 mL of pure ethanol. After a second centrifugation, the precipitate (approximately 2 mg) was freeze-dried and subsequently, enzymatic hydrolysis was performed. The precipitate (2–3 mg) was hydrolysed with beta-glucanase (2 mg) from *Trichoderma longibrachiatum* (Sigma–Aldrich) in 1 mL of 50 mM citrate buffer (pH 4.8) for 1 h at 37 °C in a water bath. The sugars released were analysed using high-performance anion-exchange chromatography (HPAE). Fourier-transform infrared spectroscopy (FT-IR) was performed placing 2–5 mg of polysaccharides on a universal attenuated total reflectance accessory (Perkin Elmer spectrum 100).

Table 4
Intracellular metabolites for trehalose synthesis, glycerol-3-phosphate and mannose-6-phosphate (m, μmol/g), experimental errors (e, %) and the difference in the specific concentration of the metabolite regarding the average of the group (D_m, %), metabolites with significantly different levels for the duplicates are indicated in blue (Tukey test with 95% confidence interval).

Conditions	Glycerol-3-phosphate			Glucose-1-phosphate			Uridine-5-diphosphoglucose		
	m	e	D_m	m	e	D_m	m	e	D_m
G101	1.985	±28.7	10.9	0.079	±15.7	7.3	1.774	±7.9	5.6
G102	2.400	±36.0	23.6	0.085	±6.2	11.6	1.481	±3.9	3.6
G201	1.671	±6.7	1.3	0.052	±20.6	12.0	1.227	±0.3	11.6
G202	0.463	±15.4	35.8	0.059	±2.4	6.9	1.905	±4.3	9.6
FG1	1.516	±45.8	3.9	0.060	±15.3	8.3	1.366	±3.3	10.2
FG2	0.720	±30.5	24.4	0.058	±15.3	9.6	1.607	±2.8	3.1
S1	1.452	±62.3	1.6	0.061	±20.5	7.4	2.098	±18.3	11.2
S2	1.937	±2.1	18.9	0.107	±9.6	25.3	1.784	±13.5	2.1
Conditions	**Trehalose-6-phosphate**			**Trehalose**			**Mannose-6-phosphate**		
	m	e	D_m	m	e	D_m	m	e	D_m
G101	0.096	±19.3	7.3	79.97	±18.3	7.8	0.561	±16.1	4.1
G102	0.063	±18.3	12.1	74.38	±14.4	10.7	0.495	±18.1	2.2
G201	0.044	±15.8	23.5	44.72	±11.1	26.4	0.458	±4.4	5.9
G202	0.131	±2.3	28.3	179.58	±0.9	44.9	0.561	±3.0	4.1
FG1	0.033	±1.6	19.9	29.02	±1.7	2.8	0.417	±6.1	16.1
FG2	0.027	±12.7	25.5	35.06	±3.4	7.0	0.585	±8.1	2.4
S1	0.101	±19.8	41.7	35.82	±1.5	8.3	0.542	±3.3	5.9
S2	0.059	±9.3	3.8	23.08	±27.1	12.5	0.913	±5.5	24.3

Samples for proton NMR analysis were prepared by using 0.2 g of LiCl in 1.0 mL D_2O, followed by 9 mL of DMSO and a few grains of deuterated (3-(trimethylsilyl)-2,2,3,3-tetradeutero propionic acid or TMSP-d4) were added. 0.5 mL of this solution was transferred to the vials containing the samples (5–15 mg). Then, they were heated in a thermo-shaker at 100 °C for 12 h. The cooled solutions were then transferred to an NMR tube and all measurements were carried out at 25 °C using an Agilent 400-MR DD2 equipped with a 5 mm OneNMR probe. The data for proton NMR spectra were collected with 1024 scans, d1 = 1s (399.7 MHz).

2.3. Extracellular glucose analysis

For the analysis of extracellular glucose, the samples were diluted with 1 M NaOH to precipitate proteins that could interfere with the analysis. Precipitated proteins were removed by centrifugation (2000x g, 10 min). The samples were analysed using high-performance anion-exchange chromatography (HPAE), Dionex ICS-5000 with PAD detector (Rohrer et al., 2013). The analysis was performed in triplicate.

2.4. Analysis of intracellular metabolites

The samples for the analysis of the intracellular metabolites of each condition came from 3 different days during the steady-state. The cells on the walls of the bioreactor were not considered influencing the specific concentrations of the metabolites since the system was very stable during the steady-state. Intracellular metabolites were extracted and analysed according to Lameiras et al. (2015). Broth (approx. 1.3 mL) was rapidly withdrawn into 10 mL of pre-cooled 40% (v/v) aqueous methanol solution (−20 °C) and after, the samples were weighted for estimation of the cell mass and kept at −20 °C until extraction of the metabolites. Methanol was removed by filtration and the samples were washed thrice with a cold methanol solution (−20 °C). Then, boiling ethanol extraction was performed to disrupt the cells and inactivate the enzymes. To this end, 25 mL of ethanol solution (75% v/v) was first pre-heated at 75 °C, whereafter the quenched and washed cell samples were added to the ethanol solution together with 100 μL of U-^{13}C-labeled cell extract of *S. cerevisiae* as the internal standard and incubated in a water bath at 95 °C for 3 min. After the extraction, the samples were first placed on ice and then stored at −80 °C.

Before the quantification of the metabolites, ethanol was evaporated until almost dryness in a Rapid-Vap under vacuum for 240 min. After evaporation, the residues were suspended in 500 μL of Milli-Q water and centrifuged at 1000x g for 5 min in a tube coupled with a filter (0.22 μm) to remove cell debris. The supernatants were stored at −80 °C until analysis. The concentrations of the intracellular metabolites were measured by isotope dilution mass spectrometry (LC-IDMS/MS and GC-IDMS) according to the protocols of Dam et al. (2002), Jonge et al. (2011) and Cipollina et al. (2009). More details of the method for the analysis of intracellular metabolites are described in Lameiras et al. (2015).

Experimental errors displayed in Tables 1–4 correspond to the standard deviation, and for Tables 5 and 6, they correspond to the standard deviation of the mean ($s_x = s/\sqrt{n}$) (Wellmer, 1998). Where s is the sample standard deviation and n is the number of the means of samples. Tables 5 and 6 show the arithmetic means (average values) of the means of samples and their corresponding standard deviation of the means.

3. Results and discussion

3.1. Analysis of intracellular metabolites

Intracellular metabolites from the tricarboxylic acid cycle, glycolysis and pentose phosphate pathway, as well as nucleotides, were quantified. Tables 1–4 show the specific concentrations of the

Table 5
Average of the concentrations of intracellular metabolites (μmol/g).

Metabolites	This work (average values)	Lameiras et al. (2015)
Glucose	3.565 ± 0.952	
Glucose-6-phosphate	1.769 ± 0.164	3.482 ± 0.131
Fructose-6-phosphate	0.385 ± 0.045	0.843 ± 0.04
Fructose-1,6-bisphosphate	0.417 ± 0.058	0.212 ± 0.023
Glyceraldehyde-3-phosphate	0.019 ± 0.003	0.018 ± 0.003
Dihydroxyacetone phosphate	0.158 ± 0.020	0.238 ± 0.025
3-phosphoglycerate	0.574 ± 0.061	0.542 ± 0.043
2-phosphoglycerate	0.056 ± 0.005	0.049 ± 0.003
Phosphoenolpyruvate	0.041 ± 0.009	0.054 ± 0.007
6-phosphogluconate	1.039 ± 0.172	0.283 ± 0.015
Ribulose-5-phosphate	0.123 ± 0.022	0.144 ± 0.003
Ribose-5-phosphate	0.325 ± 0.025	0.329 ± 0.01
Xylulose-5-phosphate	0.217 ± 0.034	0.252 ± 0.009
Sedoheptulose-7-phosphate	0.524 ± 0.044	1.102 ± 0.041
Erythrose-4-phosphate	0.004 ± 0.0005	0.008 ± 0
Citrate	13.915 ± 1.027	15.982 ± 0.723
Isocitrate	0.213 ± 0.026	0.215 ± 0.01
α-Ketoglutarate	0.616 ± 0.062	0.906 ± 0.087
Succinate	1.324 ± 0.295	0.649 ± 0.025
Fumarate	1.021 ± 0.066	0.844 ± 0.034
Malate	2.776 ± 0.202	3.203 ± 0.131
Trehalose	62.703 ± 18.229	66.73 ± 3.377
Trehalose-6-phosphate	0.069 ± 0.013	0.061 ± 0.007
Glucose-1-phosphate	0.07 ± 0.007	0.07 ± 0.004
Glycerol-3-phosphate	1.518 ± 0.229	0.147 ± 0.005
Mannose-6-phosphate	0.566 ± 0.054	
Uridine-5-diphosphoglucose	1.655 ± 0.103	
Adenosine monophosphate	0.336 ± 0.044	
Adenosine diphosphate	1.115 ± 0.110	
Adenosine triphosphate	2.964 ± 0.142	
Uridine monophosphate	0.077 ± 0.010	
Uridine diphosphate	0.128 ± 0.007	
Uridine triphosphate	0.609 ± 0.058	
Guanosine monophosphate	0.192 ± 0.034	
Guanosine diphosphate	0.206 ± 0.008	
Guanosine triphosphate	0.815 ± 0.070	

intracellular metabolites and the concentrations of extracellular glucose at the steady-state for all the conditions. It was assumed that the chemostat experiments would result in similar intracellular metabolite levels during steady-state. First of all, because the sugars used as substrates were highly similar (glucose, fructose and sucrose) and all enter the central metabolism via glycolysis. Second, because the cell growth rate was the same in all experiments (Gelain, 2020). The Tukey test with 95% confidence interval (OriginPro 8 software) was applied to analyse the average values for the replicates. The test was applied between the conditions G101 and G102, G201 and G202, FG1 and FG2, S1 and S2. Statistically significant differences in concentrations of metabolites are highlighted in blue (Tables 1–4).

The conditions evaluated were divided into two groups, first group composed of the conditions using glucose as the sole carbon source (G101, G102, G201 and G202) and the second group composed of the conditions using fructose/glucose and sucrose (FG1, FG2, S1 and S2). To verify the similarity of the values of the intracellular metabolites for each group, it was calculated how far each specific concentration of the metabolite analysed for each condition was from the average of all the conditions (Equation (1)). If all the metabolite concentrations from each group are close to the average, which would be expected, the D_m value is close to zero percent.

$$D_m(\%) = \frac{\sqrt{\frac{(m-\bar{x})^2+(Av-\bar{x})^2}{2}}}{Av}100 \quad (1)$$

Where D_m is the difference in the specific concentration of the metabolite analysed regarding the average of the conditions for each group, m is the value of the specific concentration of the metabolite analysed (Tables 1–4), Av is the average of all the specific concentrations of the metabolite analysed for each group, $\bar{x}$ is the average between m and Av. The values of D_m are presented in Tables 1–4.

3.2. Presence of extracellular polysaccharides

The presence of polysaccharides in the culture supernatant during the steady-state was confirmed through ethanol precipitation, followed by enzymatic hydrolysis for the experiments with glucose at 10 g/L (G101), sucrose (S1) and fructose/glucose (FG1). Ethanol precipitation provided a white coloured substance that was hydrolysed by beta-glucanase only generating glucose for all the samples at retention times close to 7.9 min. The release of glucose after hydrolysis of the polysaccharides suggests the presence of beta-glucans.

FT-IR analysis of the precipitates from all the conditions (Fig. 1) shows a clear peak in the region of polysaccharides (1200-900 cm^{-1}) (Thumanu et al., 2015). Proton NMR analysis was applied to obtain more information about the properties of the extracellular polysaccharides. The samples analysed were the conditions with glucose at 10 (G101) and 20 g/L (G201), fructose/glucose (FG1) and sucrose (S1). The samples presented similar profiles. Fig. 2 shows the results for the condition at 20 g/L of glucose (G201). The proton NMR spectrum of polysaccharides is mainly composed of three regions: the ring proton region (3.1–4.5 ppm); the anomeric proton region (4.5–5.5 ppm); and the alkyl region (1.2–2.3 ppm) (Ismail and Nampoothiri, 2010). The region between approximately 7 and 8 ppm could indicate the presence of aromatic compounds (Kuplich et al., 2012). Peaks corresponding to the ring proton region and one peak close to the anomeric proton region can be observed in Fig. 2.

All chemostat experiments started when the carbon source from the batch stage was depleted. For G202 condition, for example, the batch stage started with 10 g/L of glucose and, after 23 h, it was switched to continuous culture using 20 g/L of glucose in the feed. Before reaching the steady-state, a transition stage was observed (stage preceding the steady-state of CO_2 and cells). This behaviour was observed in all experiments after the batch stage. Different colours of the cells were observed for the different stages. Fig. 3 shows that the colour changed from brown-yellow to white-yellow. Although viscosity was not measured, the observed viscosity of the medium also changed, it was higher during the steady-state (C) than during the batch (A) and transition stage (B). However, the supernatant was not viscous, only with the presence of the cells the medium appeared to be more viscous.

The main reason for these alterations is probably related to the increase in the stirring speed from 200-400 rpm (batch culture) to a constant speed of 600 rpm (continuous culture). Extracellular polysaccharides were observed from the batch cultures until the steady-state of the continuous cultures. Therefore, the increase in the stirring speed did not induce the production of polysaccharides; however, this change probably influenced the colour of the pigments secreted and the structure of the polysaccharides (apparent increase in broth viscosity). The microorganism could

Table 6
Average of mass-action ratios considering all the conditions for some intracellular metabolites: 2-phosphoglycerate (2PG), 3-phosphoglycerate (3PG), Adenosine diphosphate (ADP), Adenosine monophosphate (AMP), Adenosine triphosphate (ATP), Citrate (Cit), Fructose-6-phosphate (F6P), Fumarate (Fum), Glucose-1-phosphate (G1P), Glucose-6-phosphate (G6P), Glucose (Gluc), Isocitrate (iCit), Mannose-6-phosphate (M6P), Malate (Mal), Phosphoenolpyruvate (PEP), Ribose-5-phosphate (Rib5P), Ribulose-5-phosphate (Ribu5P), Xylulose-5-phosphate (Xyl5P)

Mass-action ratio (Q)	EC number	Enzyme	Q	K_{eq} literature[a]
[G6P][ADP]/[Gluc][ATP]	2.7.1.1	Hexokinase	0.25 ± 0.05	4.7 ±0.8x10^3
[F6P]/[G6P]	5.3.1.9	Phosphohexose isomerase	0.22 ± 0.01	0.32 ±0.08
[G1P]/[G6P]	5.4.2.2	Phosphoglucomutase	0.04 ± 0.003	0.058 ± 0.003
[2PG]/[3PG]	5.4.2.1	Phosphoglycerate mutase	0.09 ± 0.01	0.092 ± 0.004
[PEP]/[2PG]	4.2.1.11	Enolase	0.72 ± 0.09	4.1 ± 0.7
[Rib5P]/[Ribu5P]	5.3.1.6	Ribose-5-phosphate isomerase	3.11 ± 0.42	3 ± 1
[Mal]/[Fum]	4.2.1.2	Fumarate hydratase	2.77 ± 0.22	4.3 ± 0.7
[Xyl5P]/[Ribu5P]	5.1.3.1	Ribulose-phosphate 3-epimerase	1.82 ± 0.06	1.7 ± 0.8
[M6P]/[F6P]	5.3.1.8	Phosphomannose isomerase	1.51 ± 0.08	0.8 ± 0.2
[iCit]/[Cit]	4.2.1.3	Aconitate hydratase	0.02 ± 0.002	0.06 ± 0.02
[ATP][AMP]/[ADP]^2	2.7.4.3	Adenylate kinase	0.86 ± 0.15	1.2 ± 0.3
[ATP]/[ADP]			2.80 ± 0.23	~ 10^{-5}
Energy charge			Value	Literature[b]
([ATP]+0.5[ADP])/([ATP]+[AMP]+[ADP])			0.80 ±0.01	0.7 - 0.95

a – Equilibrium constants (K_{eq}) reported by Canelas et al. (2011), [ATP]/[ADP] reported by Meyrat and Ballmoos (2019), and [G6P][ADP]/[Gluc][ATP] reported by Kubota and Ashihara (1990). b – Energy charge range reported by De la Fuente et al. (2014).

have changed the structure of the polysaccharides to protect the hyphae from the higher shear stress.

3.3. Evaluation of the concentrations of intracellular metabolites

The high experimental errors observed for some specific concentrations of the metabolites (Tables 1–4) can be attributed to a possible heterogeneity of cells inside the bioreactor caused by the consumption of fragments from polysaccharides, which can be released from the cell wall due to the shear stress (Rau, 1999). The bioreactor present regions with different shear levels and consequently, could also present regions with different concentrations of fragments. Thus, the cells would be in the presence of a concentration gradient of these fragments. Gentiobiose was suggested by HPAE analysis at retention times close to 32.7 min, principally for the conditions using glucose as the carbon source (Gelain, 2020). This disaccharide is probably a fragment from extracellular polysaccharides.

All the conditions were at steady-state of cell concentration and CO_2, and differences observed in Tables 1–4 can be due to the consumption of fragments from extracellular polysaccharides and the products from their hydrolysis. The changes highlighted in Tables 1–4 were not considered as resulting from sample processing and/or analytical errors due to the low experimental errors.

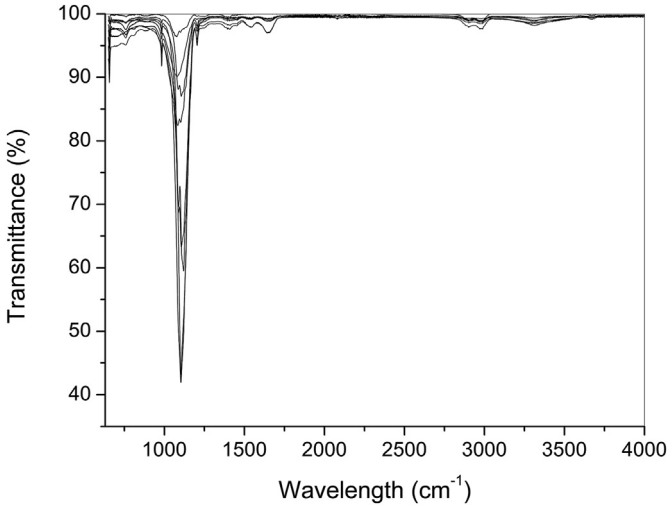

Fig. 1. FT-IR analysis of the precipitates from all the conditions (G101, G102, G201, G202, FG1, FG2, S1 and S2).

The possible influence of the consumption of fragments from extracellular polysaccharides on metabolite concentrations can be similar to what is observed in studies evaluating disturbances in the intracellular metabolism provoked by different pulses of substrates. For example, Wang et al. (2019) reported a study about the response of *A. niger* grown under glucose-limited chemostat conditions to extracellular glucose stimuli. They observed a quick response of the central carbon metabolism intermediates to both levels of glucose pulse evaluated.

A possible proof that the microorganism consumed fragments from polysaccharides is the secretion of extracellular enzymes identified by a shotgun proteomics analysis and the estimation of enzymatic activity (Gelain et al., 2020). The presence of several extracellular enzymes indicates that fragments were being consumed and they acted as inducer substrates (Gelain et al., 2020).

The microorganism consumed the carbon from the feed at a constant rate and used this carbon to synthesize components such as extracellular polysaccharides. Fragments from these polysaccharides probably started being released due to the shear stress and consumed due to the carbon-limited condition, thus creating a second carbon flow rate. Therefore, there was a possible carbon recirculation and based on the different concentrations of extracellular and intracellular glucose even for the duplicates (Table 1), the concentration of carbon was not completely stable at steady-state. This instability of carbon outside the cells could consequently have influenced the carbon flow rate into the cells.

The high values of D_m observed for several metabolites analysed including glycerol-3-phosphate, trehalose-6-phosphate, ribulose-5-phosphate and succinate indicate instability of their concentrations between the conditions of each group. Assuming that the fragments of polysaccharides contributed to increasing the experimental errors, they could also have contributed to the instability observed for the concentrations of some metabolites.

The average of the intracellular metabolites was compared with the results presented by Lameiras et al. (2015) in Table 5. These authors optimized the method used in this project for quantitative analysis of metabolites from continuous culture. Lameiras et al. (2015) presented continuous cultures using *Aspergillus niger* NW185, glucose as the carbon source and dilution rate close to the

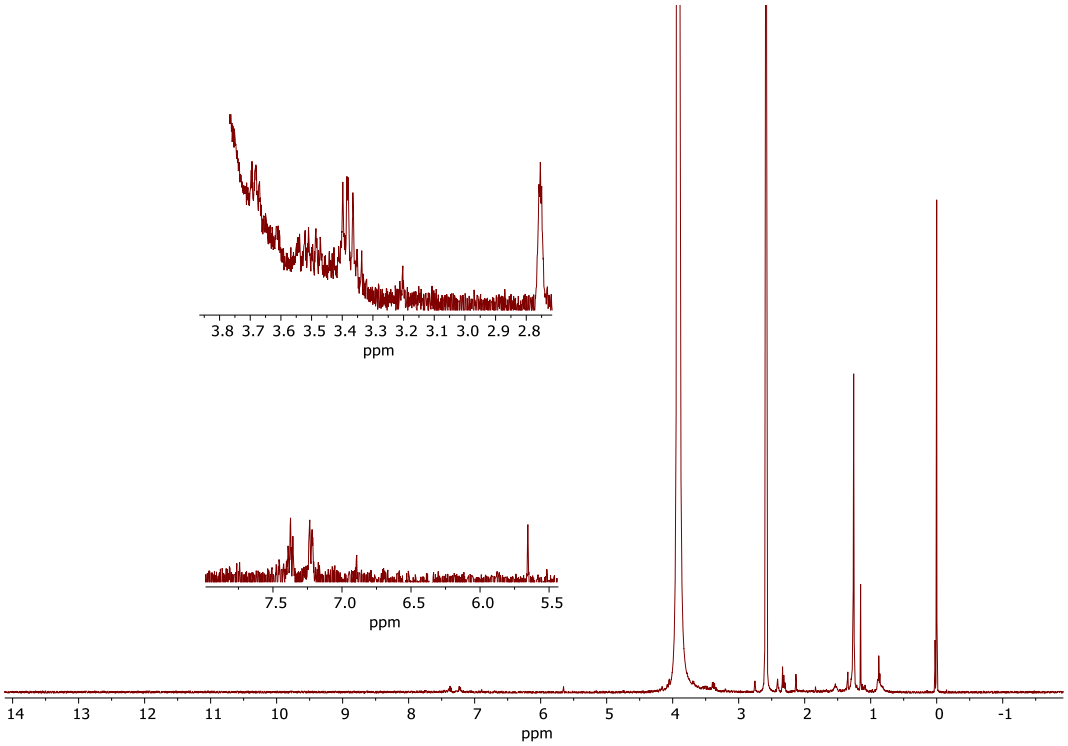

Fig. 2. Proton NMR, glucose at 20 g/L condition (G201).

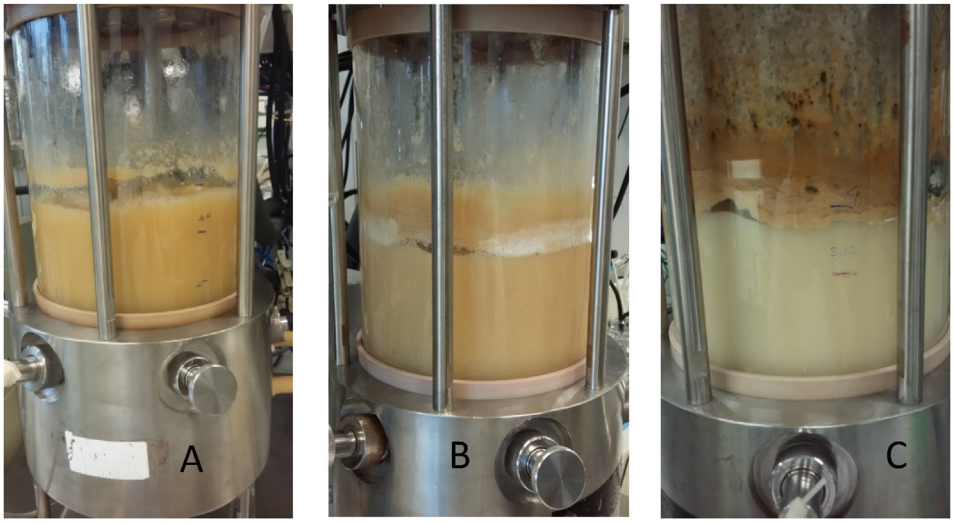

Fig. 3. Different colours between the batch (A), transition stage (B), and steady-state of cells and CO_2 (C) for G202 experiment. (For interpretation of the references to colour in this figure legend, the reader is referred to the Web version of this article.)

one used here, 0.043 h^{-1}. Interestingly, the concentrations of the majority of the metabolites (Table 5) are similar to those obtained by Lameiras et al. (2015).

To evaluate the results of the intracellular metabolites presented in Tables 1–4, it was performed analysis of the mass-action ratios for some reactions considering the average ratios of all the conditions (G101, G102, G201, G202, FG1, FG2, S1 and S2). Table 6 presents the results of mass-action ratios and indicates that the majority of the reactions analysed was close to the equilibrium, except for the [PEP]/[2PG] ratio, which was almost 6 times lower than the equilibrium. [ATP]/[ADP] ratio provides a value much far from the equilibrium due to the cell growth reactions and [G6P][ADP]/[Gluc][ATP] ratio is also far from the equilibrium providing the driving force that moves the metabolites through the glycolytic pathway (Karp, 2009). The average energy charge calculated was 0.80 ± 0.01, which is considered normal for many organisms growing under optimal conditions (De la Fuente et al., 2014).

Fragments from extracellular polysaccharides could have created an unpredictable carbon flow rate into the cells and this possible heterogeneity provided by the presence of fragments was

reflected in the different concentrations of metabolites presented in Tables 1–4 even for the duplicates (highlighted in blue in Tables 1–4). Metabolic profiles generated were influenced by a complex extracellular environment possibly containing different fragments at different concentrations; this complexity imposes difficulties to propose correlations between the metabolic profiles and the conditions.

Average values of the intracellular metabolites employing all conditions (Table 5) seem more suitable for representing the intracellular behaviour of *T. harzianum,* assuming that the concentrations of the metabolites remain within a range based on the stability provided by the steady-state (at least 6 residence times). To improve the quantification of intracellular metabolites when there is an influence of fragments from extracellular polysaccharides, more samples at different times should be taken for each sampling day during a few days, and then an average of the averages from each sampling day could be used. In this work, it was taken only one sample per sampling day for 3 days, and then it was calculated an average.

Since the presence of extracellular polysaccharides in the growth culture was never reported for the strain used, this work provides interesting data about their influence on the intracellular metabolite concentrations under carbon-limited conditions and this behaviour must be considered for the optimization of the method in future works. Additionally, an optimized method must be used to guarantee the absolute quantification of the concentrations of the metabolites employing *T. harzianum* and this will be addressed in future works.

4. Conclusions

Intracellular metabolites were analysed during the cell growth of *T. harzianum* P49P11 using different limiting carbon sources. The production of extracellular polysaccharides by *T. harzianum* P49P11 was discovered in this work. Some specific concentrations of the intracellular metabolites analysed were different regarding their duplicates and the analysis provided high experimental errors. The possible consumption of fragments from extracellular polysaccharides by the cells under carbon-limited conditions might have influenced the estimation of intracellular concentrations of the metabolites due to a possible heterogeneity of the cells inside the bioreactor. The averages of the metabolite concentrations based on the similar conditions used in this work seem more suitable for representing the metabolic profile of *T. harzianum* grown with the dilution rate of 0.05 h^{-1}. This study has provided information about the intracellular behaviour of the wild type strain *T. harzianum* and challenges of the analysis imposed by using carbon-limited conditions during the production of extracellular polysaccharides.

Acknowledgements

This project was supported by the São Paulo Research Foundation (FAPESP), process number 2014/22537-9, the University of Campinas, Delft University of Technology and the dual degree program between the University of Campinas and Delft University of Technology. The authors would like to thank Cor Ras and Patricia van Dam for the analysis of intracellular metabolites and Stephen Eustace for the NMR analysis.

References

Buchholz, A., Takors, R., Wandrey, C., 2001. Quantification of intracellular metabolites in Escherichia coli K12 using liquid chromatographic-electrospray ionization tandem mass spectrometric techniques. Anal. Biochem. 295, 129–137. https://doi.org/10.1006/abio.2001.5183.

Canelas, A.B., Ras, C., ten Pierick, A., van Gulik, W.M., Heijnen, J.J., 2011. An in vivo data-driven framework for classification and quantification of enzyme kinetics and determination of apparent thermodynamic data. Metab. Eng. 13 (3), 294–306. https://doi.org/10.1016/j.ymben.2011.02.005.

Cipollina, C., Pierick, A.T., Canelas, A.B., Seifar, R.M., Maris, A.J., Dam, J.C., Heijnen, J.J., 2009. A comprehensive method for the quantification of the non-oxidative pentose phosphate pathway intermediates in Saccharomyces cerevisiae by GC–IDMS. J. Chromatogr., B 877 (27), 3231–3236. https://doi.org/10.1016/j.jchromb.2009.07.019.

Dam, J.C., Eman, M.R., Frank, J., Lange, H.C., Dedem, G.W., Heijnen, S.J., 2002. Analysis of glycolytic intermediates in Saccharomyces cerevisiae using anion exchange chromatography and electrospray ionization with tandem mass spectrometric detection. Anal. Chim. Acta 460 (2), 209–218. https://doi.org/10.1016/S0003-2670(02)00240-4.

De la Fuente, I.M., Cortés, J.M., Valero, E., Desroches, M., Rodrigues, S., Malaina, I., Martínez, L., 2014. On the dynamics of the adenylate energy system: homeorrhesis vs homeostasis. PLoS One 9. https://doi.org/10.1371/journal.pone.0108676.

Delabona, P.S., Cota, J., Hoffman, Z.B., Paixão, D.A.A., Farinas, C.S., Cairo, J.P.L.F., Lima, D.J., Squina, F.M., Ruller, R., Pradella, J.G., 2013. Understanding the cellulolytic system of Trichoderma harzianum P49P11 and enhancing saccharification of pretreated sugarcane bagasse by supplementation with pectinase and α-L-arabinofuranosidase. Bioresour. Technol. 131, 500–507. https://doi.org/10.1016/j.biortech.2012.12.105.

Delabona, P.S., Farinas, C.S., da Silva, M.R., Azzoni, S.F., Pradella, J.G., 2012. Use of a new Trichoderma harzianum strain isolated from the Amazon rainforest with pretreated sugar cane bagasse for on-site cellulase production. Bioresour. Technol. 107, 517–521. https://doi.org/10.1016/j.biortech.2011.12.048.

Gelain, L., 2020. Mathematical modelling of cellulase production and continuous production of enzymes under carbon-limited conditions by Trichoderma harzianum P49P11. https://doi.org/10.4233/uuid:cf8840b6-c075-4e3e-af43-2b9fbc7ff0a1.

Gelain, L., Pradella, J.G.C., Costa, A.C., 2015. Mathematical modeling of enzyme production using Trichoderma harzianum P49P11 and sugarcane bagasse as carbon source. Bioresour. Technol. 198, 101–107. https://doi.org/10.1016/j.biortech.2015.08.148.

Gelain, L., Pabst, M., Pradella, J.G.C., Costa, A.C., van der Wielen, L., van Gulik, W.M., 2020. Analysis of the proteins secreted by Trichoderma harzianum P49P11 under carbon-limited conditions. J. Proteom. 227, 103922. https://doi.org/10.1016/j.jprot.2020.103922.

Gientka, I., Błażejak, S., Stasiak-Różańska, L., Chlebowska-Śmigiel, A., 2015. Exopolysaccharides from yeast: insight into optimal conditions for biosynthesis, chemical composition and functional properties – review. Acta Sci. Pol. Technol. Aliment. 14 (4), 283–292. https://doi.org/10.17306/J.AFS.2015.4.29.

Ismail, B., Nampoothiri, K.M., 2010. Production, purification and structural characterization of an exopolysaccharide produced by a probiotic Lactobacillus plantarum MTCC 9510. Arch. Microbiol. 192, 1049–1057. https://doi.org/10.1007/s00203-010-0636-y.

Jonge, L.P., Buijs, N.A., Pierick, A.T., Deshmukh, A., Zhao, Z., Kiel, J.A., Heijnen, J.J., van Gulik, W.M., 2011. Scale-down of penicillin production in Penicillium chrysogenum. Biotechnol. J. 6 (8), 944–958. https://doi.org/10.1002/biot.201000409.

Jonge, L.P., Douma, R.D., Heijnen, J.J., van Gulik, W.M., 2012. Optimization of cold methanol quenching for quantitative metabolomics of Penicillium chrysogenum. Metabolomics 8, 727–735. https://doi.org/10.1007/s11306-011-0367-3.

Karp, G., 2009. Cell and Molecular Biology: Concepts and Experiments, sixth ed. J. Wiley, New York, p. 108.

Kubota, K., Ashihara, H., 1990. Identification of non-equilibrium glycolytic reactions in suspension-cultured plant cells. Biochim. Biophys. Acta 1036, 138–142. https://doi.org/10.1016/0304-4165(90)90025-R.

Kuplich, M.D., Grasel, F.S., Campo, L.F., Rodembusch, F.S., Stefani, V., 2012. Synthesis, characterization and photophysical properties of ESIPT reactive triazine derivatives. J. Braz. Chem. Soc. 23, 25–31. https://doi.org/10.1590/S0103-50532012000100005.

Lameiras, F., Heijnen, J.J., van Gulik, W.M., 2015. Development of tools for quantitative intracellular metabolomics of Aspergillus Niger chemostat cultures. Metabolomics 11 (5), 1253–1264. https://doi.org/10.1007/s11306-015-0781-z.

Li, H., Yu, H., Zhu, H., 2017. Structure studies of the extracellular polysaccharide from Trichoderma sp. KK19L1 and its antitumor effect via cell cycle arrest and apoptosis. Appl. Biochem. Biotechnol. 182 (1), 128–141. https://doi.org/10.1007/s12010-016-2315-1.

Mahapatra, S., Banerjee, D., 2013. Fungal exopolysaccharide: production, composition and applications. Microbiol. Insights 6, 1–16. https://doi.org/10.4137/MBI.S10957.

Meyrat, A., von Ballmoos, C., 2019. ATP synthesis at physiological nucleotide concentrations. Sci. Rep. 9 (1), 3070. https://doi.org/10.1038/s41598-019-38564-0.

Pinu, F.R., Villas-Boas, S.G., Aggio, R., 2017. Analysis of intracellular metabolites from microorganisms: quenching and extraction protocols. Metabolites 7, 53. https://doi.org/10.3390/metabo7040053.

Rau, U., 1999. Production of schizophyllan. In: Bucke, C. (Ed.), Carbohydrate Biotechnology Protocols. Humana Press Inc., Totowa, pp. 48–55.

Rohrer, J.S., Basumallick, L., Hurum, D., 2013. High-performance anion-exchange chromatography with pulsed amperometric detection for carbohydrate analysis of glycoproteins. Biochemistry 78, 697–709. https://doi.org/10.1134/S000629791307002X.

Thumanu, K., Sompong, M., Phansak, P., Nontapot, K., Buensanteai, N., 2015. Use of infrared microspectroscopy to determine leaf biochemical composition of cassava in response to Bacillus subtilis CaSUT007. J. Plant Interact. 10 (1), 270–279. https://doi.org/10.1080/17429145.2015.1059957.

Wang, S., Liu, P., Shu, W., et al., 2019. Dynamic response of Aspergillus Niger to single pulses of glucose with high and low concentrations. Bioresour. Bioprocess. 6, 16. https://doi.org/10.1186/s40643-019-0251-y.

Wellmer, F.-W., 1998. Statistical Evaluations in Exploration for Mineral Deposits. Springer-Verlag Berlin Heidelberg, p. 41.